33rd Annual International Conference of the IEEE EMBS
Boston, Massachusetts USA, August 30 - September 3, 2011

Ambiguity and Regularization in Parallel MRI

Derya Gol, Lee C. Potter
Deparment of Electrical & Computer Engineering and Davis Heart & Lung Institute
The Ohio State University, Columbus, OH, 43210

***Abstract*—In this paper, we formulate the parallel magnetic resonance imaging(pMRI) as a multichannel blind deconvolution problem with subsampling. First, the model allows formal characterization of image solutions consistent with data obtained by uniform subsampling of k-space. Second, the model allows analysis of the minimum set of required calibration data. Third, the filter bank formulation provides analysis of the sufficient sizes of interpolation kernels in widely used reconstruction techniques. Fourth, the model suggests principled development of regularization terms to fight ambiguity and ill-conditioning; specifically, subspace regularization is adapted from the blind image super-resolution work of Sroubek et al. [11]. Finally, characterization of the consistent set of image solutions leads to a cautionary comment on $L1$ regularization for the peculiar class of piece-wise constant images. Thus, it is proposed that the analysis of the subsampled blind deconvolution task provides insight into both the multiply determined nature of the pMRI task and possible design strategies for sampling and reconstruction.**

I. Introduction

Parallel Magnetic Resonance Imaging (pMRI) provides fast imaging of soft tissues with the parallel use of phased-array coils. The spatial diversity of coil sensitivity profiles serves to augment phase encoded gradients for achieving spatial localization; using fewer phase-encoding steps accelerates data acquisition. Many image reconstruction algorithms has been proposed, including SENSE [1], SMASH [2] and GRAPPA [3]. SENSE unfolds spatial aliasing in the image domain, while SMASH is a k-space method that estimates the non-acquired k-space points from the acquired ones. Each of these methods assume that the coil sensitivity information is available; however, coil sensitivities are generally unknown and must be estimated. To estimate them, autocalibration methods have been proposed, such as AUTO-SMASH [4] and GRAPPA, where extra central k-space lines are acquired.

Interpreted in k-space, each channel provides sub-Nyquist samples of the convolution of the unknown image with a coil sensitivity. If the sensitivities are assumed to be perfectly known, then the pMRI problem can be modeled as a filter-bank problem, as described in [8] and [9], and several methods given in digital communication literature (e.g. [10]) can be applied to find perfect reconstruction filters.

In the case of unknown coil sensitivities, the pMRI problem can be fundamentally modeled as a blind multi-channel deconvolution (BMD) problem with sub-sampling. Related work in optical imaging considers similar challenges under the name of blind super-resolution [11]; and, without subsampling the multi-channel deconvolution has been explored in wireless communications. The EVAM [5] subspace technique is a well-known BMD concept that has been applied to the pMRI problem [6], albeit with no subsampling. Similarly [7] also invoked EVAM results for the estimation of coil sensitivities when autocalibration lines provide a reference image.

In this paper, we first characterize the solutions consistent with the k-space data, revealing the multiply determined nature of the task. We assume that both the sensitivities and the image are deterministic but unknown, and that k-space data are uniformly downsampled in the phase encoding direction. In addition, the smoothness of coil sensitivities in the image domain is exploited by modeling their k-space representations as having small support (FIR filters). A polyphase decomposition is used to describe the non-uniqueness of images consistent with all data in the ideally noiseless case. Knowledge of the set of all solutions motivates selection of regularization terms to augment the non-convex least-square data fitting, thereby combating both local minima and non-unique global minima.

II. Problem Formulation

In pMRI, the continuous-parameter k-space signal is simultaneously acquired by K coils

$$g_i(k) = \int_{FOV} \rho(r) c_i(r) e^{j2\pi kr} dr, \tag{1}$$

where r is the 3D spatial position, $\rho(r)$ is the unknown spin magnetization of the object to be imaged, $c_i(r)$ denotes the i^{th} coil sensitivity, and $g_i(k)$ is the k-space data for $i = 1, ..., K$. Here, FOV refers to the field of view. Eq. 1 can be written as the convolution of Fourier transform of spin magnetization $f(k)$ with the Fourier transform of coil sensitivities $s_i(k)$.

$$g_i(k) = \int_{-\infty}^{\infty} f(\nu) s_i(k-\nu) d\nu. \tag{2}$$

The imaged object has finite spatial support, so the convolution result in Eq. 2 must formally have an infinite support. Practically, we truncate this support to capture any desired arbitrarily large fraction of the energy. For simplicity, we proceed below in two spatial dimensions, $r = (x, y)$ and sample at locations $(k_x, k_y) = (m\nabla k_x, n\nabla k_x)$. Then, we denote the Nyquist-sampled version of Eq. 2 as

$$g_i(m, n) = s_i(m, n) * f(m, n), \tag{3}$$

where $*$ is the linear convolution operation. Next, we subsample by rate R in the phase-encoding direction, k_x. Let D denote this uniform subsampling in the k_x index.

$$g_i = D(s_i * f). \tag{4}$$

Coil sensitivities are widely reported as smoothly varying spatial functions; therefore, we model the corresponding k-space sensitivities as FIR filters, meaning that s_i is non-zero only at low spatial frequencies. Denoting the these FIR models as h_i, then they may be written as

$$s_i(m,n) = \sum_{u=-\lfloor M/2 \rfloor}^{\lceil M/2 \rceil - 1} \sum_{v=-\lfloor N/2 \rfloor}^{\lceil N/2 \rceil - 1} c_i(u,v) e^{j2\pi(\frac{mu}{M}+\frac{nv}{N})}, \quad (5)$$
$$h_i = s_i(-\lfloor \frac{m_h}{2} \rfloor : \lceil \frac{m_h}{2} \rceil - 1, -\lfloor \frac{n_h}{2} \rfloor : \lceil \frac{n_h}{2} \rceil - 1),$$

where $\lfloor . \rfloor$ and $\lceil . \rceil$ refer to the floor and ceiling operations on real numbers. Here, each coil sensitivity function is modeled by $m_h \times n_h$ non-zero low-pass k-space samples. Because convolution is a linear operation, we can write Eq. 4 in matrix form by vectorizing $f(m,n)$ into a single MN-by-1 vector

$$g_i = DC_{h_i} f, \quad i = 1, ..., K. \quad (6)$$

Each $C_{h_i}, \quad i = 1, ..., K$ is a 2D convolution matrix having a Toeplitz-block-Toeplitz (TBT) structure. The size of each C_{h_i} matrix is $((m_h + M - 1)(n_h + N - 1), MN)$.

Thus, we have a subsampled blind multi-channel deconvolution signal model, because both the image and coil sensitivities are unknown. Owing to the subsampling, the C_{h_i} matrices are not convolutions; consequently, we put Eq. 6 into polyphase decomposition, following e.g. [11], to analyze solutions. In brief, polyphase representation allows the decimated output to be written as the sum of convolutions with decimated versions of the input. The p^{th} polyphase component of g_i is obtained by taking every R^{th} sample starting from p. That is,

$$g_i^p(m,n) = g_i(mR + p, n), \quad p = 0, ..., R-1,$$

and similarly for the filters, h_i. Thus, in polyphase form,

$$\begin{bmatrix} g_1^0 \\ g_2^0 \\ \vdots \\ g_K^0 \end{bmatrix} = \begin{bmatrix} C_{h_1}^{00} & C_{h_1}^{01} & \cdots & C_{h_1}^{0,(R-1)} \\ C_{h_2}^{00} & C_{h_2}^{01} & \cdots & C_{h_2}^{0,(R-1)} \\ \vdots & \vdots & \ddots & \vdots \\ C_{h_K}^{00} & C_{h_K}^{01} & \cdots & C_{h_K}^{0,(R-1)} \end{bmatrix} \begin{bmatrix} f^0 \\ f^1 \\ \vdots \\ f^{(R-1)} \end{bmatrix}, \quad (7)$$

where $C_{h_i}^{j,k}$ is the convolution matrix of h_i^{j-k}. Thus, each coil's downsampled k-space data can be written in k-space as the sum of filtered versions of the downsampled image,

$$g_i^0 = \sum_{p=0}^{R-1} f^p * h_i^{-p}. \quad (8)$$

The downsampled coil data are the first polyphase component of the fully-sampled k-space. This polyphase decomposition results in the multiple-input, multiple-output (MIMO) convolution model depicted in Fig. (1) for subsampling $R = 3$ and $K = 4$ coils. Each solid line into a summation represents a polyphase filter component, h_i^{-p}, for i^{th} coil and p^{th} polyphase component.

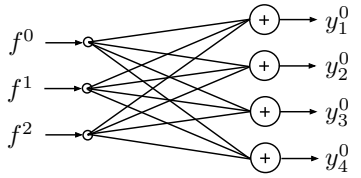

Fig. 1. A MIMO interpretation arises from polyphase decomposition of the pMRI signal model; the representation is illustrated here for subsampling $R = 3$ and $K = 4$ coils.

III. Solutions are Not Unique

Using Eq. 7, we explore the set of all solutions that are consistent with the downsampled, multi-channel k-space data. The multiply determined nature of the image recovery task then is used to motivate a regularized inversion strategy.

From Eq. 7 we can immediately observe that any image consistent with the decimated k-space data is accompanied by an R-dimensional space of solutions. Specifically, let f and $\{h_i\}$, $i = 1, ..., K$, solve Eq. 4. Then we can choose R arbitrary non-zero complex scalars $\alpha = \{\alpha_1, ..., \alpha_R\}$ and scale each polyphase component to obtain another solution f' for the image and h' for coil sensitivities:

$$f' = \sum_{p=0}^{R-1} \alpha_p f^p, \quad h_i' = \sum_{p=0}^{R-1} \frac{1}{\alpha_p} h_i^p. \quad (9)$$

This is evident in Fig. (1) in that any scale factor can be incorporated either in the unknown input, or in the unknown filters that operate on that input. Further, from the downsampled k-space measurements, y_i^0, the ordering of the R polyphase components of f is ambiguous. Thus, any of R factorial permutations of the polyphase components is consistent with the observed data.

Proposition 1. *Suppose that f is any solution to Eq. 4. Then, there exists an infinite number of solutions including*

$$\sum_{p=0}^{R-1} \alpha_p f^{\Pi(p)},$$

where α_p is any non-zero complex scalar, $p = 0, \cdots, R-1$ and Π is any permutation on the indices $\{0, \cdots, R-1\}$.

Moreover, additional solutions are given by adopting R equal and opposite shifts in the polyphase components of the image and coil sensitivities. Thus, even in the noiseless setting, any effort to uniquely recover an image solely from the k-space samples is futile due to the ambiguities. Additional restrictions, based on physical characteristics of the true image or true coil sensitivities, are required. This holds for any $R \geq 2$, regardless of the number of coils, K.

To illustrate the ill-posed nature of pMRI from uniform downsampling, Fig. 2 displays three images that are consistent with k-space data; the example is computed for $M = N = 64$, $K = 6$, and $R = 2$. Fig. 2b is obtained from scaled versions of polyphase components where $\alpha_1 = 0.5$ and $\alpha_2 = 1.5$,

and Fig. 2c shows the resulting image where the polyphase components are permuted.

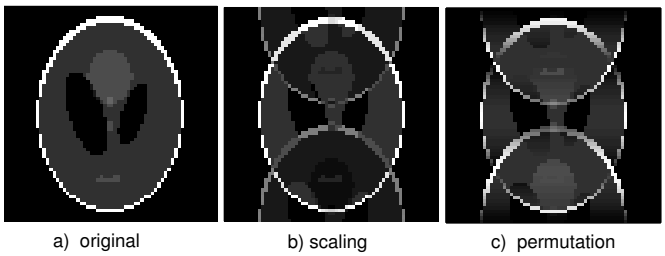

Fig. 2. Illustration of the ill-posedness of pMRI from uniform downsampling. Panels (a-c) each provide a data-matching image for sub-sampled k-space data with downsampling $R = 2$ and $K = 6$ coils.

In addition, the size of the solution set can grow if f is not uniquely determined for a *known* set of coil sensitivities. The next proposition provides necessary and sufficient conditions for the linear equations in Eq. 7 to have rank MN for fixed h_i, and hence to yield unique f for known sensitivities.

Proposition 2. *The linear equations in Eq. 7 have full column rank only if $K \geq R$ and $m_h \geq R$. The equations are full rank if and only if $K \geq R$ and all R-by-R minors of the K-by-R polynomial matrix of sensitivity polyphase components have non-zero determinant [10].*

Similarly, we can characterize uniqueness of coil sensitivities for a known image. By the commutativity of convolution, Eq. 6 can be written as

$$g_i = DC_f h_i, \quad i = 1, ..., K, \tag{10}$$

where C_f is convolution matrix constructed using the known image, f. We again use a polyphase decomposition. Stacking data from polyphase components of all K coils gives

$$g^P = (I \otimes C_f^0) h^P, \tag{11}$$

where $\otimes$ is Kronecker product operation and I is an identity matrix. The size of C_f^0 is $(\lceil \frac{m_h+M-1}{R} \rceil (n_h + N - 1), m_h n_h)$.

Proposition 3. *For a known image, the linear equations in Eq. 11 can have full column rank, and hence give unique coil sensitivities, only if $M \geq R$ and $\lceil \frac{m_h+M-1}{R} \rceil (n_h + N - 1) \geq m_h n_h$.*

The second inequality in Prop. 3 merely states that rows are no fewer than the columns; a sufficient condition is $N \geq \frac{m_h n_h}{\lceil \frac{M}{R} \rceil}$.

Definition 1. *If a property of a vector $v \in \mathbb{R}^n$ fails to hold only on a closed set of zero measure that is nowhere dense in $\mathbb{R}^n$, then the property is said to hold for* generic v.

Remark 1. *Under the size conditions in Propositions 2 and 3, Equations 7 and 11 are full rank for generic h and f.*

Propositions 1-3 exemplify insights found by casting the pMRI problem in the filter bank framework. In addition, existing results from the MIMO systems literature provide formal results on sufficient sizes of equalization kernels and interpolation kernels [10]. Further, the framework allows formal proof that $R - 1$ calibration lines are generically both necessary and sufficient to eliminate, in the noiseless case, all image ambiguity due to subsampling. Next, we use the filter bank framework to suggest a regularization term.

IV. Subspace Constraint on Coil Sensitivities

In this section, we provide one regularization term that restricts the unknown filters h_i to a low-dimensional subspace. Our development is motivated by the EVAM principle (e.g., [5], [7]) and follows the treatment for image subsampling given by Sroubek et al. [11]. Upon decimation, we have only the zeroth polyphase component of the output, g_i^0. We seek a bank of nullifying filters

$$\sum_{i=1}^{K} (g_i^0 * \eta_i) = \sum_{i=1}^{K} (G_i^0 \eta_i) = \mathcal{G}\eta = 0, \tag{12}$$

where G_i^0 is a convolution matrix of g_i^0. Thus, the nullifying filter vector η lies in the null space of $\mathcal{G} = F\mathcal{H}$ [11] where

$$\mathcal{H} = \begin{bmatrix} C_{h_1}^{00} & C_{h_2}^{00} & \cdots & C_{h_K}^{00} \\ C_{h_1}^{10} & C_{h_2}^{10} & \cdots & C_{h_K}^{10} \\ \vdots & \vdots & \ddots & \vdots \\ C_{h_1}^{(R-1),0} & C_{h_2}^{(R-1),0} & \cdots & C_{h_K}^{(R-1),0} \end{bmatrix}, \tag{13}$$

and F is the convolution matrix of f. Then, if F has full rank, the null-spaces of $\mathcal{G}$ and $\mathcal{H}$ are equal. Therefore, the nullifying filters can also be used to nullify the unknown filters vector h for generic f. From (noiseless) data, we can construct $\mathcal{G}$ and the projection $\mathcal{N}$ onto the null-space of $\mathcal{G}$, yielding the following requirement on the unknown filters:

$$\mathcal{N}h = 0. \tag{14}$$

Modifying the argument in [11] for our subsampling by R in the encoding dimension, we learn that the dimension of the null-space of $\mathcal{G}$ is generically R^2. Hence, although the projection $\mathcal{N}$ does not define a one-dimensional subspace containing the filters, is does provide a low-dimensional subspace. Penalizing distance of a conjectured h from this subspace can therefore provide a useful regularization term [11] to augment a norm on data mismatch.

V. Optimization Problem

Common practice is to augment k-space data with additional calibration lines, and interpolate unknown k-space data after solving a regularized least-squares problem for the interpolation kernels. Here, we illustrate use of the proposed regularization by directly solving for the unknown image; the unknown coil sensitivities as computed as a byproduct. Generally, calibration lines would be also used, and the unknown coil sensitivities require fewer unknowns than interpolation filters. In this short paper, however, we use a computed example

without calibration lines to also provide a cautionary example regarding $L1$ regularization. Specifically, it can be shown that for a noiseless piece-wise constant phantom with few jumps, the ambiguous solutions characterized in Proposition 1 all have total variation (TV) norm greater than or equal to the true phantom. Consider image reconstruction via the nonlinear, non-convex optimization problem

$$\min_{f,h} \sum_{i=1}^{K} \|g_i - DC_{h_i} f\|_2^2 + \beta_1 \|\mathcal{N}h\|_2^2 + \beta_2 TV(f) + \beta_3 TV(h). \quad (15)$$

The initial term in Eq. 15 is a data fidelity term; the first regularization term exploits the low-dimensional filter subspace sketched in Section IV. A TV norm is used as the second regularization term to exploit piecewise smoothness of an image while preserving edges (e.g., [13]–[15]). Likewise, the third regularization term exploits smoothness in the coil sensitivities. The TV norm is defined as,

$$TV(f) = \sum \sqrt{|\nabla_x \mathcal{F}(f)|^2 + |\nabla_y \mathcal{F}(f)|^2},$$

where $\mathcal{F}$ represents Fourier Transform operator which is used to pass to image domain.

For the minimization of this cost function, we simply used an Alternating Minimization (AM). In an AM method, as one variable (image or coils) is kept fixed, the minimization is computed with respect to other variable. In this case, the energy function takes a quadratic form with fixed f or h. Therefore, a descent algorithm, such as conjugate gradients, can be used to estimate the unknowns. In our simulations, we used an open-source TV minimization code [17].

For simulation, a 64-by-64 Shepp-Logan phantom [16] is used for $K = 6$ channels. To compute simulated coil sensitivities, the Biot-Savart law is applied for FOV of 40 cm in each dimension, a coil radius of 5 cm, and 20cm distance from the center of FOV to the coils. From Nyquist rate k-space sampling, the encode direction was downsampled by a factor of $R = 2$. To model k-space sensitivity functions, the size of each FIR filter was chosen as $m_h = n_h = 9$. The regularization coefficients are chosen as $\beta_1 = 1$, $\beta_2 = 6\times10^{-5}$ and $\beta_3 = 8\times10^{-3}$. Fig. 3 shows the simulation results. As it is

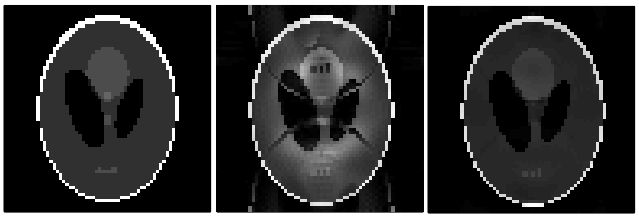

Fig. 3. Experiment results for 6-channel simulated data. (a) original image, (b) reconstructed image with no regularization, (c) reconstructed image with regularization

seen in Fig. 3b, if no regularization term is used, then aliasing and weighting error are strongly evident in the reconstructed image.

VI. Conclusion

We propose that MIMO filter banks provide a valuable viewpoint for the formal analysis of pMRI. The analysis provides necessary conditions for successful image recovery, yields results on sizes of interpolation filters, informs the minimum number of required calibration lines, and reveals a regularization term apparently new to the pMRI application. The algebraic analysis for uniform subsampling may be extensible to arbitrary k-space sampling patterns. We believe that the filter bank formulation not only illuminates current practice of k-space interpolation for pMRI, but points to the more parsimonious approach of direct equalization to estimate a single k-space image.

References

[1] K. P. Pruessmann, M. Weiger, M. B. Scheidegger, P. Boesiger, "SENSE: Sensitivity Encoding for Fast MRI," *Magn Reson Med.*, 42:952-962, 1999.

[2] D. K. Sodickson, W. J. Manning, "Simultaneous Acquisition of Spatial Harmonics (SMASH): Fast Imaging with Radiofrequency Coil Arrays," *Magn Reson Med.*, 38:591-603, 1997.

[3] M. A. Griswold, P. M. Jakob, R. M. Heidemann, M. Nittka, V. Jellus, W. Jianmin, B. Kiepfer, A. Haase, "Generalized autocalibrating partially parallel acquisitions (GRAPPA)," *Magn Reson Med.*, 47:1202-1210, 2002.

[4] P. M. Jakob, M. A. Griswold, R. R. Edelman, D. K. Sodickson, "AUTO-SMASH: A Selfcalibrating Technique for SMASH Imaging," *MAGMA*, 7:42-54, 1998.

[5] M. I. Gurelli, C. I. Nikias, "EVAM: An eigenvector-based algorithm for multichannel blind deconvolution of input colored signals," *IEEE Trans. Signal Processing*, vol 43, no 1, pp.134-149, 1995.

[6] H. She, R. R. Chen, D. Liang, Y. Chang, L. Ying, "Image Reconstruction from Phased-array MRI Data Based on Multichannel Blind Deconvolution," *7th IEEE International Symposium on Biomedical Imaging*, pp.760-763, 2010.

[7] R. L. Morrison, M. Jacob, M. N. Do, "Multichannel Estimation of Coil Sensitivities in Parallel MRI," *4th IEEE International Symposium on Biomedical Imaging*, pp.117-120, 2007.

[8] L. Ying, E. Abdelsalam, "Parallel MRI Reconstruction: A Filter-Bank Approach," *Engineering in Medicine and Biology Society 27th Annual Conference*, pp.1374-1377, 2006.

[9] Z. Chen, J. Zhang, S. Li, and L. Chai, "FB analysis of PMRI and its application to H_∞ optimal SENSE reconstruction," in *Proc. IEEE Inter. Conf. Image Proc. (ICIP)*, pp.129-132, 2007

[10] R. Rajagopal, L. C. Potter, "Multi-channel multi-variate equalizer design," *Multidimensional Systems and Signal Processing*, vol. 14, pp. 105-118, 2003.

[11] F. Sroubek, G. Cristobal, J. Flusser, "A Unified Approach to Superresolution and Multichannel Blind Deconvolution," *IEEE Transactions on Image Processing*, vol.16, no.9, pp.2322-2332, 2007.

[12] K. P. Pruessmann, "Encoding and reconstruction in parallel MRI," *NMR in Biomedicine*, 19:288-299, 2006.

[13] L. Rudin, S. Osher, E. Fatemi, "Nonlinear total variation based noise removal algorithms," *Physica D*, 60:259-268, 1992.

[14] D. Strong, T. Chan, "Edge-preserving and scale-dependent properties of total variation regularization," *Institute of Physics Publishing: Inverse Problems*, 19:S165-S187, 2003.

[15] T. Chan, C. K. Wong, "Total Variation Blind Deconvolution," *IEEE Transactions on Image Processing*, Vol.7, No:3, pp.370-375, 1998.

[16] M. Guerquin-Kern, F. I. Karahanoglu, D. Van De Ville, K. P. Pruessmann, M. Unser, "Analytical Form of Shepp-Logan Phantom For Parallel MRI," *7th IEEE International Symposium on Biomedical Imaging*, pp. 261-264, 2010.

[17] M. Tao, J. Yang, "Alternating Directions Algorithm for Total Variation Deconvolution in Image Reconstruction," TR0918, Department of Mathematics, Nanjing University, China, Aug. 2009.